11-1-1989

Crevice Corrosion Mechanism for 1018 Steel in Neutral, Acidic and Chloride Environments

M. Ingle

M. L. White

Richard D. Granata

Henry Leidheiser Jr.

ADVANCED TECHNOLOGY FOR
LARGE
STRUCTURAL SYSTEMS

Lehigh University

CREVICE CORROSION MECHANISM FOR 1018 STEEL IN NEUTRAL, ACIDIC AND CHLORIDE ENVIRONMENTS

by

M. Ingle
M.L. White
R.D. Granata
H. Leidheiser, Jr.

ATLSS Report No. 89-15

November, 1989

An NSF Sponsored Engineering Research Center

THE MECHANISM OF CREVICE CORROSION OF 1018 STEEL IN NEUTRAL, ACIDIC AND CHLORIDE ENVIRONMENTS

ABSTRACT

The crevice corrosion behavior of 1018 steel in water, 3% NaCl and pH 4.5 H_2SO_4 was studied by means of model crevices with gaps of 0.025 - 0.55 mm. Alternate wetting and drying cycles were used. The corrosion product formed in the crevice exerted a force of 1.5×10^7 Pa (2100 psi). The rapid rate of corrosion during the early stages decreased as the corrosion product impeded ingress of electrolyte as shown by impedance measurements. The pH within the crevice during the early stages was alkaline. After corrosion product formed within the crevice, the pH became acidic during each drying portion of the wet/dry cycle.

M. Ingle
M.L. White
R.D. Granata
H. Leidheiser, Jr.

The authors' research was done as a cooperative effort involving the ATLSS Center, the Department of Chemistry, and the Zettlemoyer Center for Surface Studies. Mr. Ingle is a former ATLSS graduate student who has completed his studies. M.L. White is a research scientist, retired. R.D. Granata is a senior research scientist. H. Leidheiser, Jr. is ALCOA Professor of Chemistry.

INTRODUCTION

Structures exposed to the atmosphere typically have crevices formed between the members in a connection. These connections trap moisture, dirt and salt, creating an aggressive environment in the crevice that promotes severe corrosion. This insidious attack is difficult to detect, and may destroy the integrity of critical supports. Crevice corrosion degrades the integrity of joints between mild steel members through both metal loss and corrosion-product induced pressure. Crevice corrosion decreases the effective thickness of structural members and increases the net section stress in the steel.

The severe structural problems attributed to crevice corrosion in mild steels are described by the term "packout". The iron ions formed when mild steel corrodes in atmospheric environments react with atmospheric oxygen to form insoluble iron oxides. This ion to oxide conversion is associated with a volumetric expansion of 2.4 - 4 times the initial volume of the base metal [1,2]. In an enclosed space such as a crevice, the expansion is inhibited and the resulting pressures can reach thousands of pounds per square inch (psi) [3,4].

The published literature dealing with crevice corrosion of mild steel is limited. Studies of passivating metals typically deal with systems such as 304 stainless steel in 3.5% NaCl or pure aluminum in .05M NaCl [7]. These latter metal/electrolyte systems have a different mechanism of crevice corrosion. The metal exposed to the bulk solution is passivated by the available oxygen while the metal exposed to the small volume of electrolyte trapped in the crevice actively corrodes. This concept cannot be directly applied to crevice corrosion of mild steel in sodium chloride solutions because this system does not exhibit passivity under normal service conditions.

The research described in this report was conducted to understand better the crevice corrosion of mild steel in chloride-containing environments.

EXPERIMENTAL PROCEDURE

Three types of experiments were performed and different specimens were used in each study. All three types of experiments did, however, share similar geometries, materials and assembly techniques.

The metal segments of all three designs were fabricated from one billet of hot rolled 1018 construction grade stock. In order to duplicate the conditions of the materials used in the construction of large structures such as bridges and buildings, the material received no special treatments prior to use. The 1018 steel was tested in order to determine electrochemical uniformity in the following way. Both lateral and transverse 1 cm^2 sections were cut from the billet. A wire was soldered to the back of each cm^2 sample before the samples were cast in cold mount epoxy. After curing, the samples were ground to a uniform 600 grit surface. Combinations of these lateral, and transverse samples were coupled in 3% NaCl solution for 24 h and the potential difference was determined. The majority of the samples was electrochemically uniform, with no reproducible galvanic couple effects between samples from different regions of the billet. The only reproducible galvanic couple developed when a sample from the outermost region of the billet was connected to a sample from the core. Metallographic examination of these two samples showed elongated small grains at the edge of the billet and slightly larger uniform grains through the rest of the stock. In order to eliminate chemical or structural differences, the billet was reduced by machining to either 25 or 50 mm (1000 or 2000 mils) outside diameter. The composition of the material is given in Table I.

Table I

1018 Stock Composition

Element	Specified Range (ASM)	Measured % Alloy Element
C	0.15-0.20	0.19
Mn	0.60-0.90	0.65
Si	< 0.60	0.15
P	0.035 Max	0.03
S	0.04 Max	0.03
Cu	< 0.6	0.4
Cr, Ni, Mo	NA	Trace

A clear hard acrylic material (trademark, ACRYCAL) was used for the non-metallic structural portions of the apparatus. This material was assembled using solvent (methylene chloride) bonding. The steel sections were fixed to each other and to the apparatus with an epoxy adhesive (LORD 321) free of metallic reinforcement and specifically formulated to resist environmental attack. Samples showing significant corrosion at the joint between the epoxy and the steel were eliminated.

Experimental samples were cylinders 25 or 50 mm in diameter and 50 mm long. The crevice gap ranged from 0.025 mm to 2.54 mm.

Dimensional Change Specimen

The purpose of these experiments was to determine if the corrosion product buildup in the crevice produces measurable deformation and if the initial gap size is related to the magnitude of the deformation. The specimen (Fig. 1) consisted of a steel cylinder mounted in an inert support structure. Both the flat surface and the 1018 steel cylinder were ground to a 600 grit finish before assembly and a jig was used in the grinding to ensure a sharp

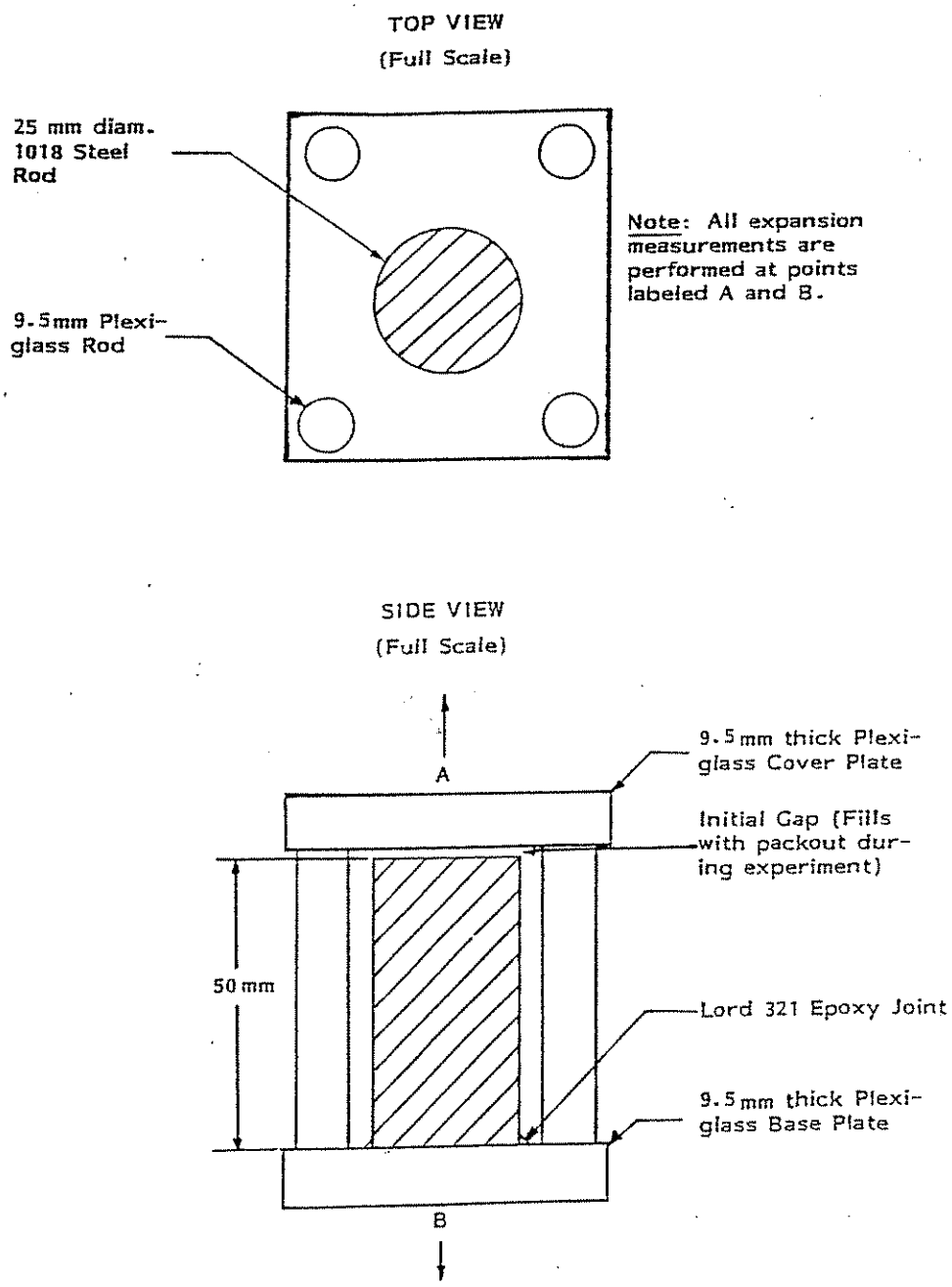

Fig. 1. Dimensional Change Measurement Specimen Sketch

edge.

After cleaning in inhibited 1,1,1-trichloroethylene vapor, the 1018 steel cylinders were mounted in epoxy on one side of the support, leaving a crevice between the other end of the steel cylinder and the cover plate. The inert ACRYCAL frame for the sample was assembled first, leaving one of the end plates free to slide on the four guide rods. The cylinder was set into epoxy on this free end plate. While the epoxy was still soft, the end plate was placed back on the guide rods. By sliding this end plate on the guide rods, the crevice end of the cylinder was brought into contact with the ACRYCAL crevice cover plate at the other end of the steel cylinder. Because the epoxy was still soft while this operation was performed, inaccuracies in the assembly were compensated by shifting of the steel specimen in the epoxy. The coplanarity of the crevice surfaces was checked using an industrial projection shadowgraph to ensure that the sample faces were within 0.02 degrees.

Mylar shims were used to set the crevice gap. Two shims were placed between the cover plate and the steel cylinder and the cylinder was brought into contact with the shims. In this configuration, the guide rods were bonded to the back cover plate using a solvent before removing the shims. Bonding required approximately 30 h.

The specimens were subjected to cyclic exposure to 3% NaCl solution. The cycle began with immersion in 3% NaCl for 24 h. The crevice was wetted manually using both syringes and vacuum in order to avoid air entrapment in the crevice. The sample was removed after 24 h and placed in a sealed chamber at 98% relative humidity and 21°C for 24 h. These cycles were repeated continuously for up to 2500 h. The clear cover plate over the crevice allowed a photographic record of the corrosion process to be obtained. Changes in dimension were measured using a calipers type micrometer (accuracy ±0.0005 in. or 0.01 mm) in order to determine the effects of the corrosion product.

Measurements were collected from two sides of each sample and averaged. In order to avoid experimental errors based on the placement of the calipers, the specimens were marked with specific measurement locations. The specimens were always measured during the dry portion of the cycle.

Inaccuracies caused by swelling of the polymeric structural components were corrected for by running control samples along with the corroding specimens. The control specimen was identical to the corroding specimens except for the use of an inert metallic cylinder.

Electrochemical Measurement Apparatus

The dimensional changes associated with corrosion packout are integrated measurements reflecting the effects of many wet/dry cycles. In order to learn more about what happens during the wet/dry cycle, a sample capable of measuring electrochemical parameters *in situ* was designed. The specimen shown in Fig. 2 incorporated design features from the apparatus used by Turnbull [6], Alavi and Cottis [7], Silverman and Krisher [8], and Alkire et al. [9].

The current measurements [8] were performed using Teflon-coated wire leads that were soldered to the bottom of each of the steel segments. The leads extended from the steel specimen through a substantial layer of epoxy and out of the specimen chamber. The current flow between the inner and outer steel segments was measured with a Keithley 385 picoammeter. A Ag/AgCl flat-faced pH reference electrode was utilized to measure the potential at the center of the crevice.

Impedance Measurement Apparatus

The electrochemical impedance spectroscopy (EIS) measurements were performed on the type of specimen shown in Fig. 3. The 50 mm diameter crevice in this case is formed between a circular cover plate and a flat epoxy mount

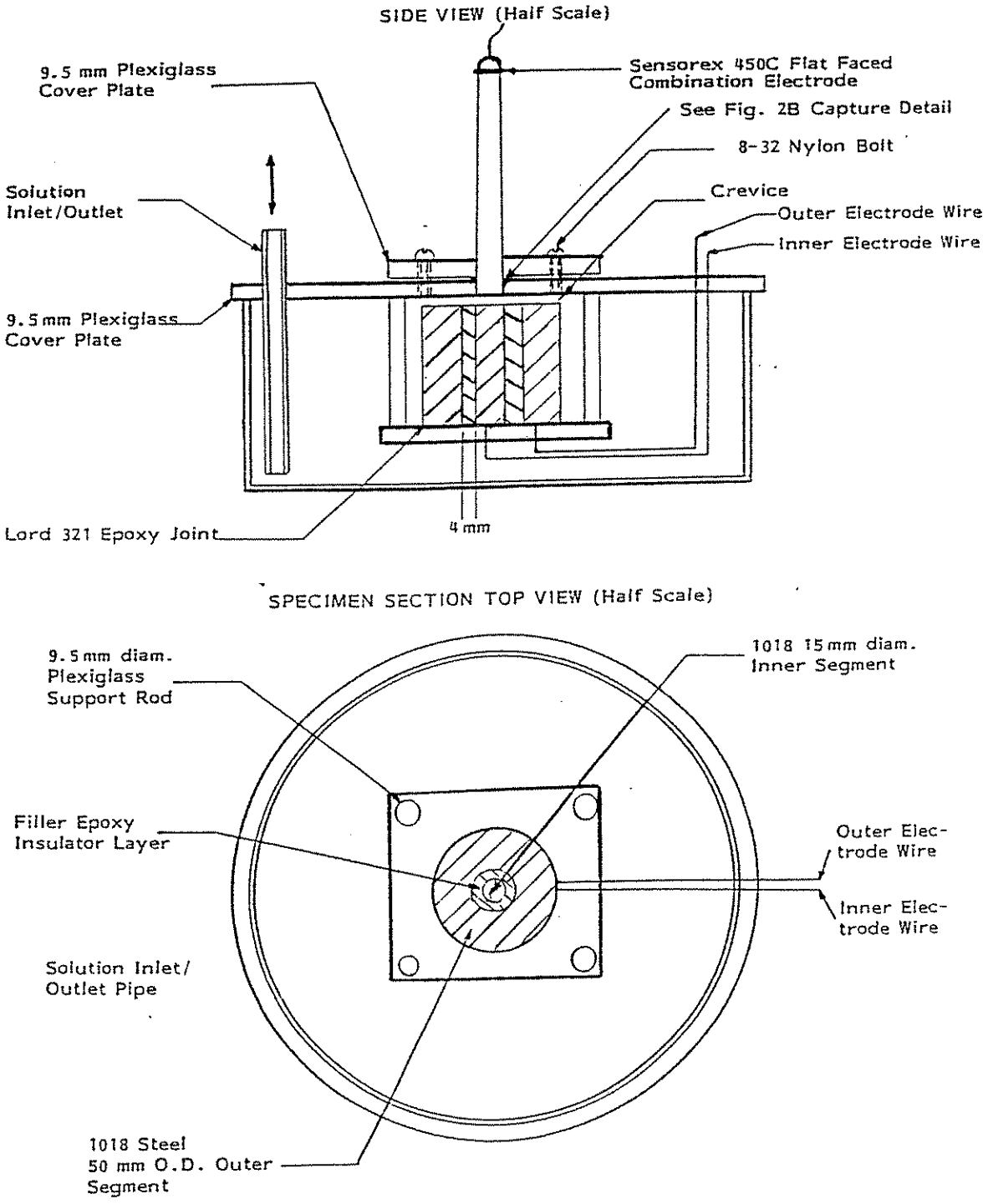

Fig. 2. Electrochemical Measurement Apparatus.

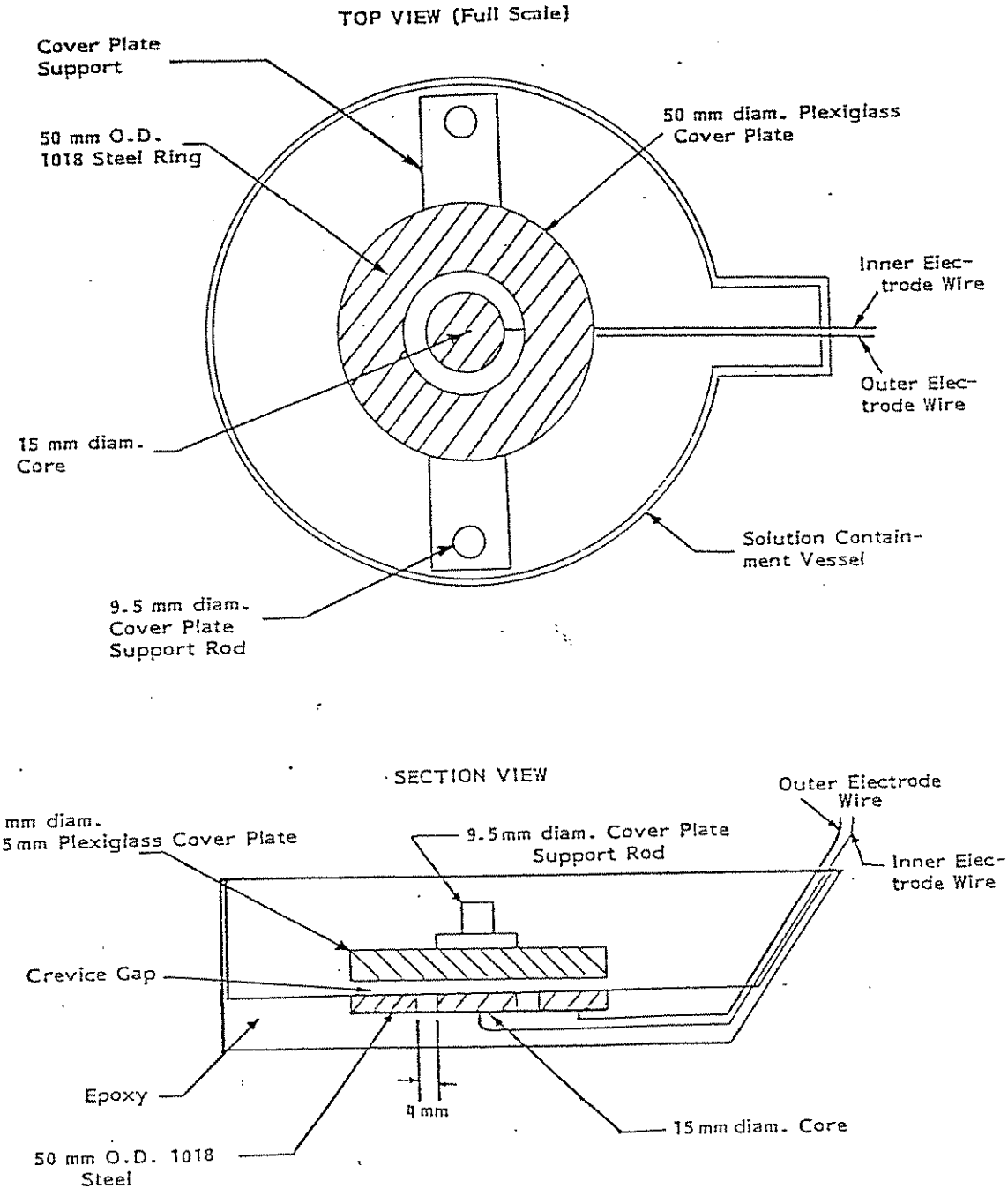

Fig. 3. Alternating Current Impedance Measurement Apparatus.

containing the two cylindrical steel electrodes. This flush mount maintains geometric consistency with the earlier specimens. Teflon-coated wires were soldered to the back of each steel electrode and submerged in the casting epoxy. Samples used in the EIS measurements had gaps from 0.02 to 2.3 mm (1-90 mils).

RESULTS AND DISCUSSION

Specimens, 25 and 50 mm in diameter, with initial gaps ranging from 0.02 to 0.5 mm (1 to 20 mils) were subjected to the 4 day/1 day wet/dry cycle in a 3% NaCl electrolyte. The data shown in Figs. 4 and 5 suggest that there is no appreciable aspect ratio effect within the range studied.

The maximum changes in dimension of these samples were used to calculate the pressures caused by corrosion products in the crevice. Figure 5 shows that the sample with the 0.3 mm gap experienced 0.45 mm of dimensional change over the course of the experiment. Assuming the load causing this deformation was evenly applied to the four rods in the apparatus, and knowing the mechanical properties of ACRYCAL (E = 2.9 GPa) and steel (E = 220 GPa), it was calculated that the pressure exerted was 1.5×10^7 GPa (2100 psi).

The pressure developed in this worst case analysis was used as a basis for comparisons with results derived from other studies of corrosion-product induced deformation. Fisher and Pense [3] in their analysis of the Mianus River bridge failure reported maximum crevice pressures near 2000 psi. Brockenbrough [4] also measured crevice pressures between 1500 and 2000 psi.

The results shown in Figs. 4 and 5 suggest that there is a change in the rate of corrosion product induced pressure over the course of the experiment. Comparing the instantaneous slopes of the data curves in the early (<1000 h) period with the same curves at the end of the experiment (2500 h), it is apparent that the rate of corrosion product build-up in the crevice is more rapid in the first 1000 h of the experiment than in the next 1500 h. This effect is consistent with visual and photographic observations. During the first 1000 h, the crevice becomes packed with enough corrosion product to prevent visual assessment of the corrosion in the crevice. This correlation between the advent of a crevice packed with corrosion product and a decrease

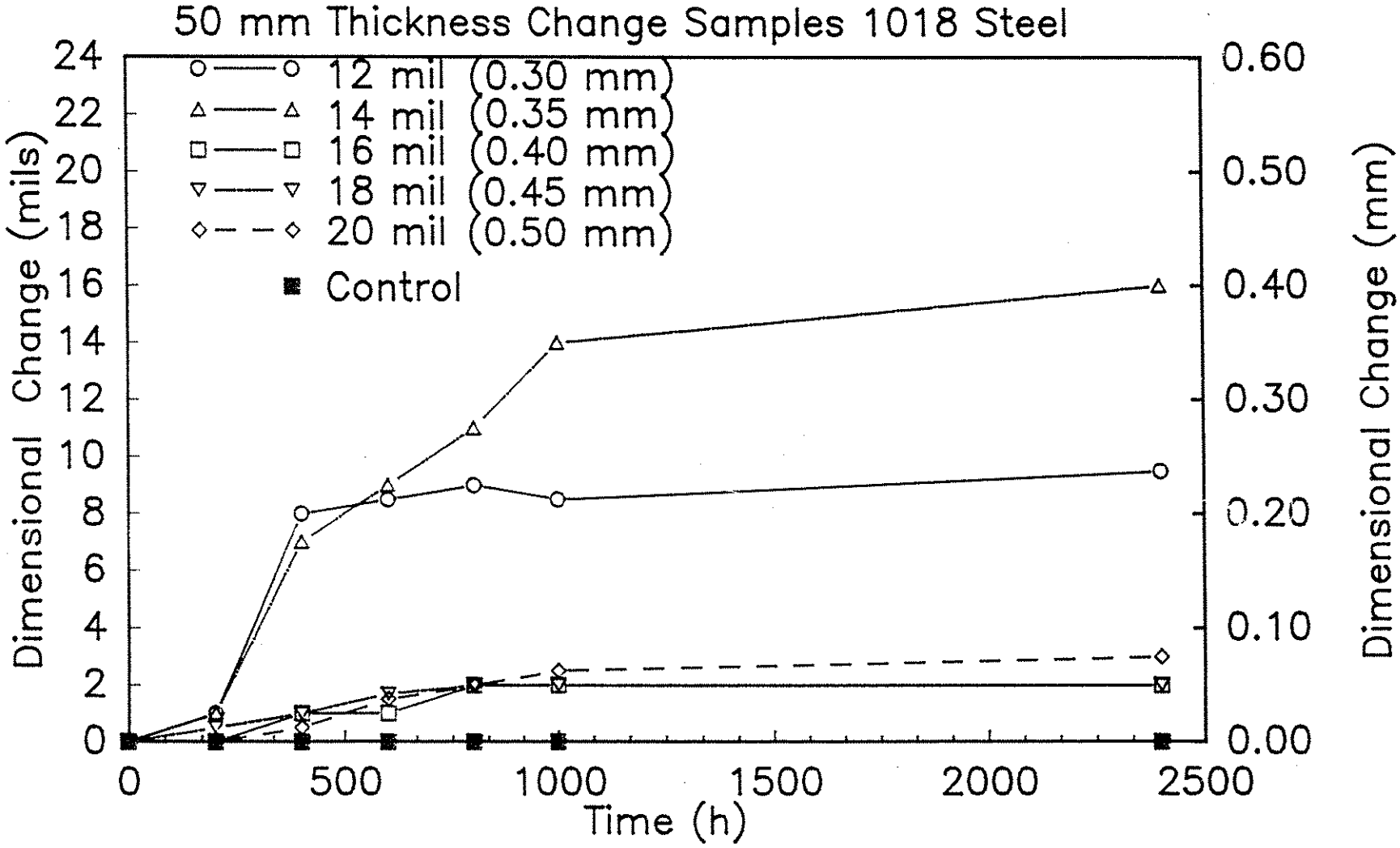

Fig. 4. Dimensional changes as a function of time for 50 mm diameter specimens subjected to 4/1 (wet/dry) cycles in 3% NaCl.

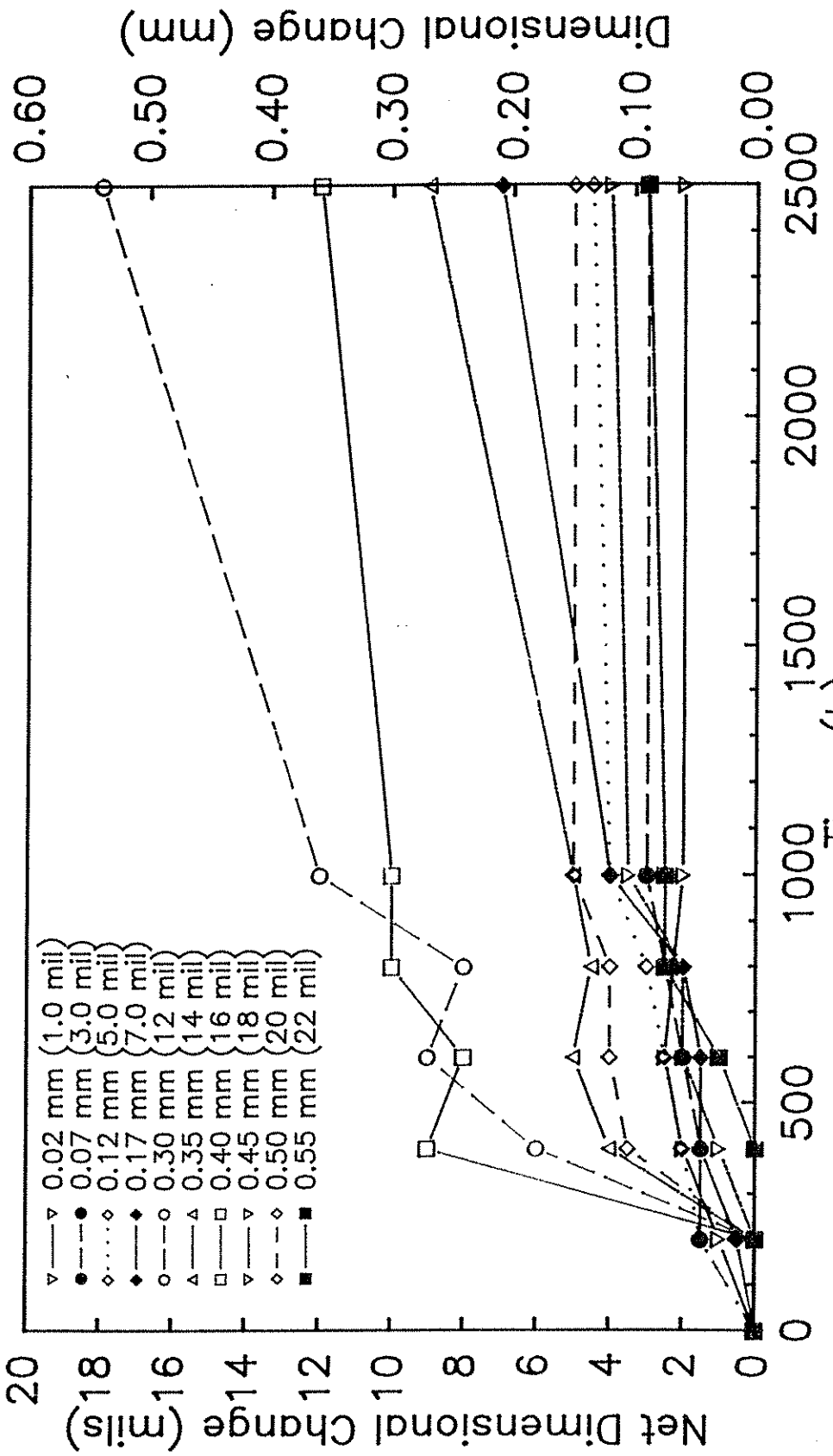

Fig. 5. Dimensional changes as a function of time for 25 mm diameter specimens subjected to 4/1 (wet/dry) cycles in 3% NaCl.

in the rate of dimensional changes in the specimens is significant and has been observed by others. In a study related to the impedance measurement of a porous magnetite film on carbon steel, Macdonald and Park [11] described the accelerated corrosion in the <1000 h time frame with the term "autocatalytic corrosion process." A reason for the slowing of the dimensional change is inhibited electrolyte transport through the corrosion-product-filled crevice as shown by impedance measurements to be described later.

The larger the initial gap setting, the greater the volume of oxides required to fill the crevice. The probability of finding defects that will allow mass transport increases with increase in gap width. This probability concept leads to the conclusion that the chances of a crevice with a small initial gap filling with a layer of corrosion product that completely inhibits transport are much greater than the chances of a large crevice becoming filled with a completely restrictive layer. Because the smallest gap specimens have the greatest chances of building up a coherent layer of corrosion product in the crevice, it may be expected that dimensional changes for these specimens will approach a limiting value at an earlier time. None of the crevice specimens with initial gap settings below 0.25 mm (10 mils) showed a positive slope in the range of 1000 to 2500 h.

The data in Fig. 6 show that the greatest change in dimension of the specimen holder assemblies at both 1000 and 2500 h occurs in the specimens with gap settings between 0.25 and 0.35 mm (10-15 mils). The maxima occurred at earlier times in the case of specimens with smaller initial gap settings.

The deformation of the specimens with smaller gaps in times less than 200 h is related to the ability of the smaller gap crevices to fill with corrosion product very quickly. Unlike a fully wet experiment in which the initial crevice gap controls the volume of electrolyte and the amount of oxygen in the crevice, the drying cycles ensure that atmospheric oxygen has access to

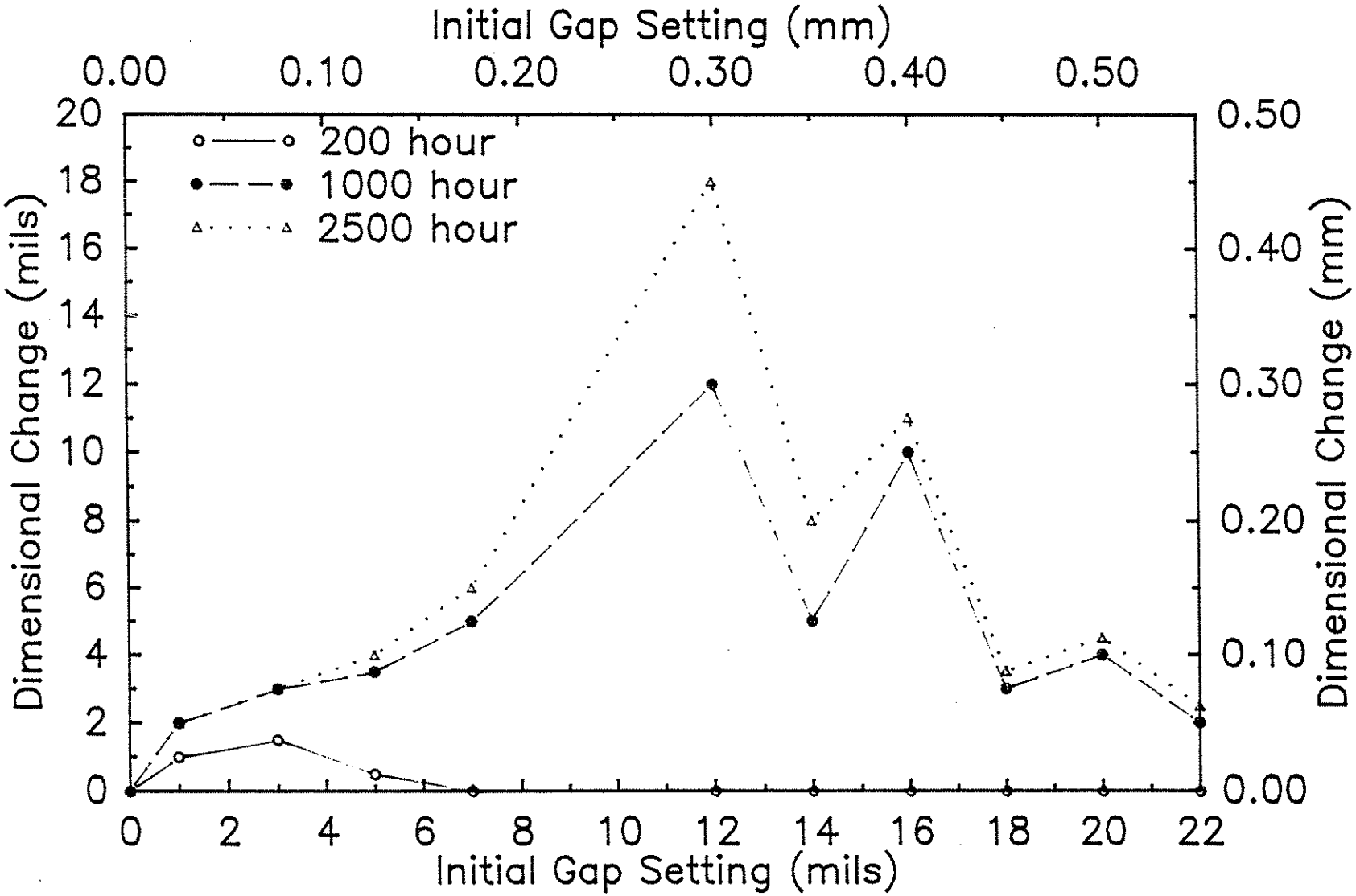

Fig. 6. Dimensional changes as a function of initial gap setting for 25 mm diameter specimens over selected time intervals.

the crevice. During a drying cycle, the electrolyte in the largest and the smallest crevices partially drains or the water partially evaporates. The uniform oxygen access leads to a uniform corrosion rate in the early stages of all of the experiments. Because a uniform corrosion rate will fill the smaller gap specimens first, it is apparent that they would be the first to exhibit measurable deformation. These small crevice gap specimens are also the first to experience the transport restrictions described above. These smaller gap specimens fill with corrosion product first, but then experience transport restrictions that limit further crevice corrosion.

The data points at 600 and 800 h for the 0.30 mm (12 mil) specimen indicate that the specimen experienced a decrease in gap dimension. This effect was observed to a lesser degree in other specimens and is not attributed to measurement error. These relaxations in the specimen can be directly related to the observed morphology of the corrosion product. The observed relaxation in the specimen may be accounted for by the following series of events. Brittle ridges of corrosion product, similar to tubercle walls, build up quickly and start to deform the assembly. A slight vibration, or disturbance from electrolyte flow during wetting (perhaps from handling during measurement) causes a brittle failure in the ridge. The elastic properties of the assembly draw back on the collapsed corrosion product ridges and cause the apparatus to experience a net decrease in dimension. As these building/collapsing cycles continue, the debris from the collapsed tubercle ridges, as well as newly formed ridges, eventually fill the crevice and promote more uniform corrosion product induced dimensional changes.

The significant deformation of the specimens with intermediate gaps ranging from 0.25 to 0.35 mm (10 to 14 mils) may be explained as a tradeoff between two conflicting effects in the crevice. The small crevices have so little volume that they quickly fill with enough corrosion product to inhibit

electrolyte transport into the crevice zone. The transport restrictions created by the corrosion product slow the rate of additional crevice corrosion. The large crevices offer little support for the fragile corrosion product ridges. The ridges collapse before they fill the corrosion gap. The corrosion products in the larger gap specimens do not create pressure in the crevice. Intermediate gap specimens are filled with enough corrosion product to deform the sample but the corrosion product layer is still thick enough to contain defects. These defects provided paths for electrolyte to travel through the oxide to the active sites at the metal surface.

Distilled water and pH 4.5 H_2SO_4 electrolytes produced little attack in the crevice relative to 3% NaCl. The pH 4.5 sulfuric acid and the distilled water electrolytes caused less deformation because they did not promote the rapid development of strong, solid corrosion product in the crevice. Figs. 7-9 show EIS data from three geometrically similar specimens with intermediate initial gap crevices that were subjected to distilled water, 4.5 pH sulfuric acid solution and 3% NaCl solutions. The data were collected after the first drying cycle at an elapsed time of approximately 140 h. The impedance behavior of the samples exposed to distilled water and 4.5 pH sulfuric acid remained the same over long times. The impedance behavior of the samples exposed to 3% NaCl changed greatly over time and will be discussed later.

The similarity in the response of the distilled water and pH 4.5 sulfuric acid trials is apparent. The log |Z| component, and the phase angle data for both electrolytes show a flat response from 0.001 Hz to 1000 Hz. It is well known that a flat response in the log |Z| data and a 0° phase angle shift is representative of a resistor [14]. Thus, the sample behaves as a resistor when subjected to low frequency. Above 1000 Hz, the specimens begin to show a decrease in the real component (Log |Z|) and a corresponding change in the phase angle to approximately -90°. The negative -90° phase angle is

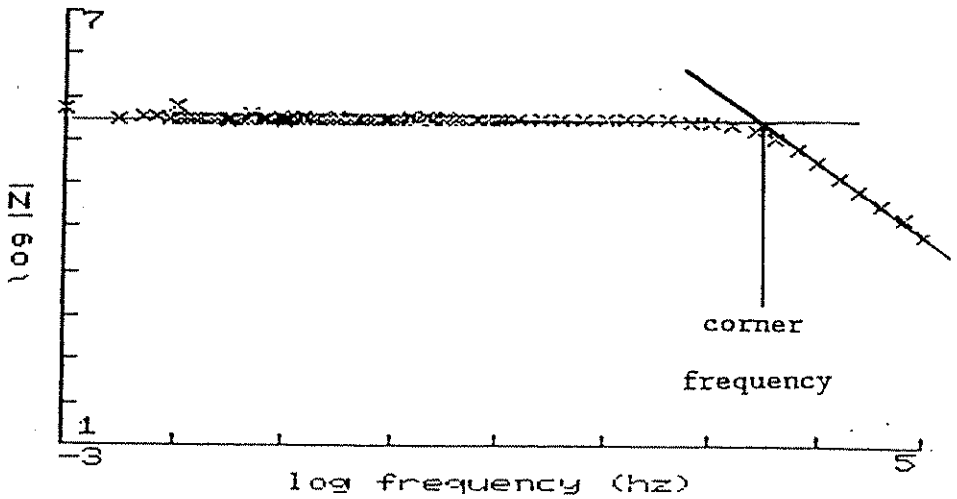

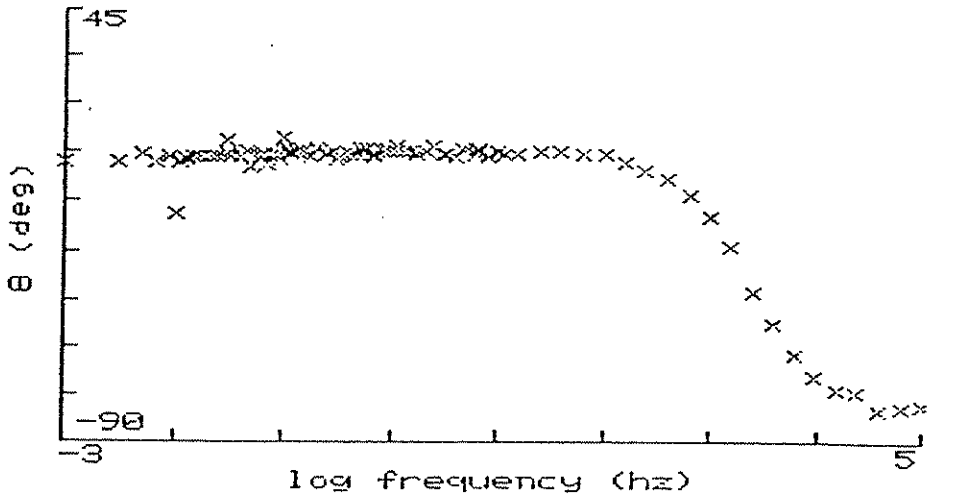

Fig. 7. Impedance data from a 0.38 mm (15 mil) gap specimen subjected to a 4/1 (wet/dry) cycle in distilled water.

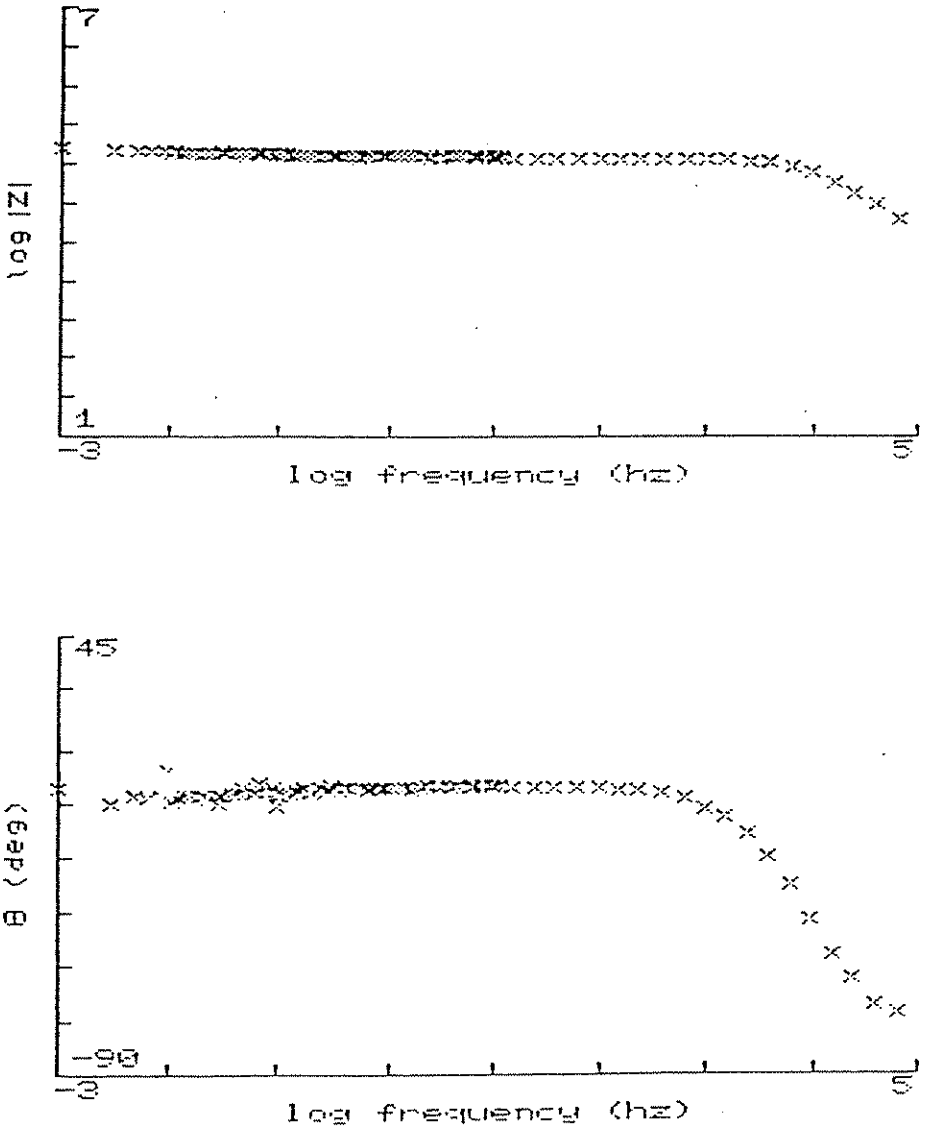

Fig. 8. Impedance data from a 0.38 mm (15 mil) initial gap specimen subjected to 4/1 (wet/dry) cycles in pH 4.5 sulfuric acid solution.

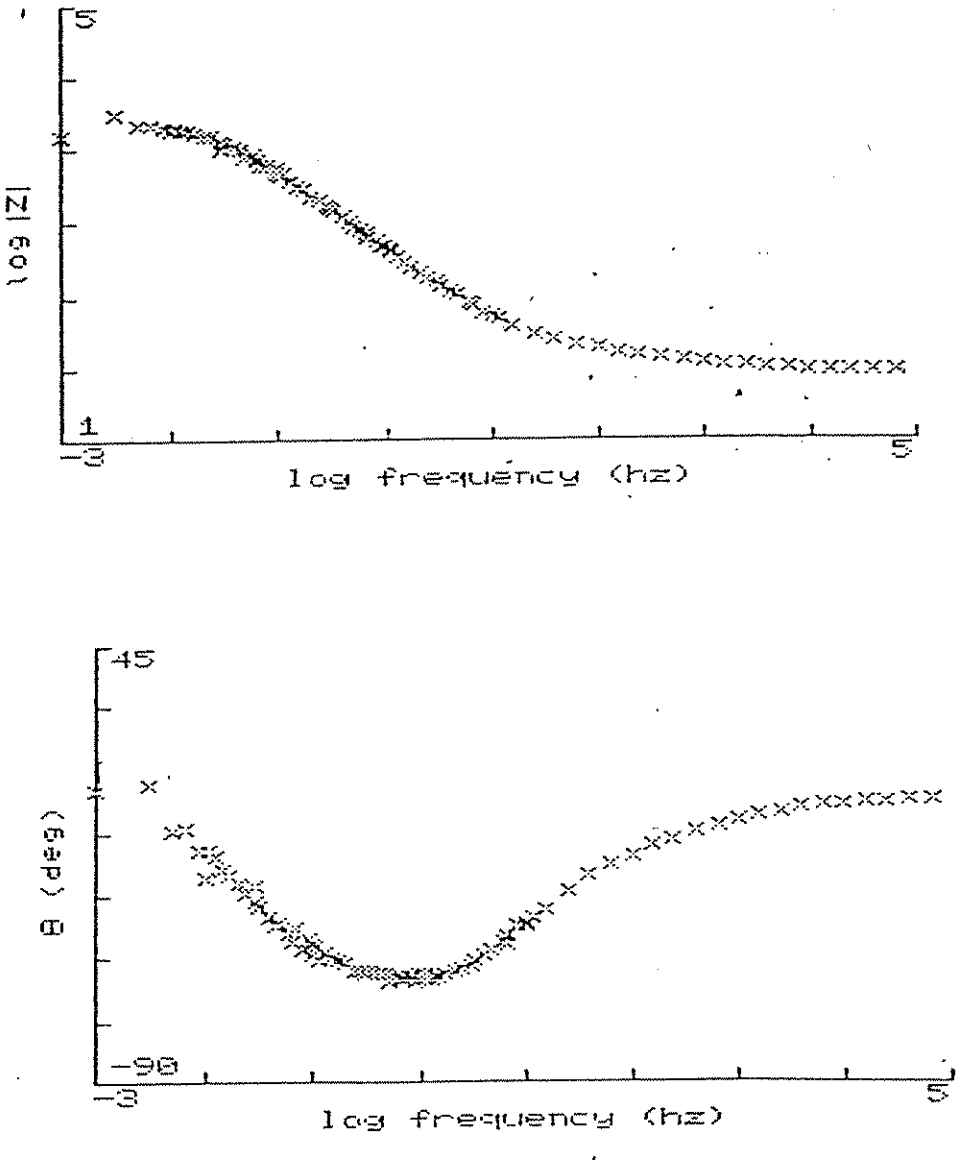

Fig. 9. Impedance data from a 0.30 mm (12 mil) initial gap specimen subjected to 4/1 (wet/dry) cycles in 3% NaCl solution.

indicative of a capacitive system [14]. The low frequency resistance in distilled water was 307,000 Ω, while the resistance in pH 4.5 sulfuric acid resistance was 92,300 Ω. The lower resistance in the pH 4.5 sulfuric acid trial signifies that the interelectrode charge transfer resistance and the transfer resistances at the electrodes are lower than the same resistances in distilled water.

The log |Z| component from the 3% NaCl trials is less than 1/10 of the magnitude of log |Z| data from the pH 4.5 sulfuric trial. The phase angle curves are also different. The 3% NaCl data are not dominated by the large resistive region seen in distilled water and pH 4.5 sulfuric acid. There is also no frequency range over which the data for 3% NaCl become totally capacitive: The phase angle was approximately -60°, not the -90° that would be expected for a pure capacitor. Thus, the oxide layer formed in this case is far less capacitive than the oxide layers formed in either the distilled water or the pH 4.5 sulfuric acid and must contain more defects.

Impedance data for a specimen having a 0.3 (12 mil gap) mm gap are presented in Fig. 10. All measurements were performed after the sample had been subjected to wet/dry cycling and were wet for at least 4 h.

Macdonald and Park [11] studied the formation of magnetite crystals in the high chloride concentration region near the annulus of a tube sheet. The circuit model developed was based on active sites with a capacitive and resistive component at the tip of a corroding crevice. The active site is separated from the bulk solution potential by a long conducting path through the electrolyte-filled pores that formed in the crystalline magnetite. The current passing through the pore leaks out through the sides of the magnetite pore in the same way current leaks from a long transmission line. The effect of the limited volume on mass transport and the effect of having to pass current from one electrode to another through a porous, electrolyte-

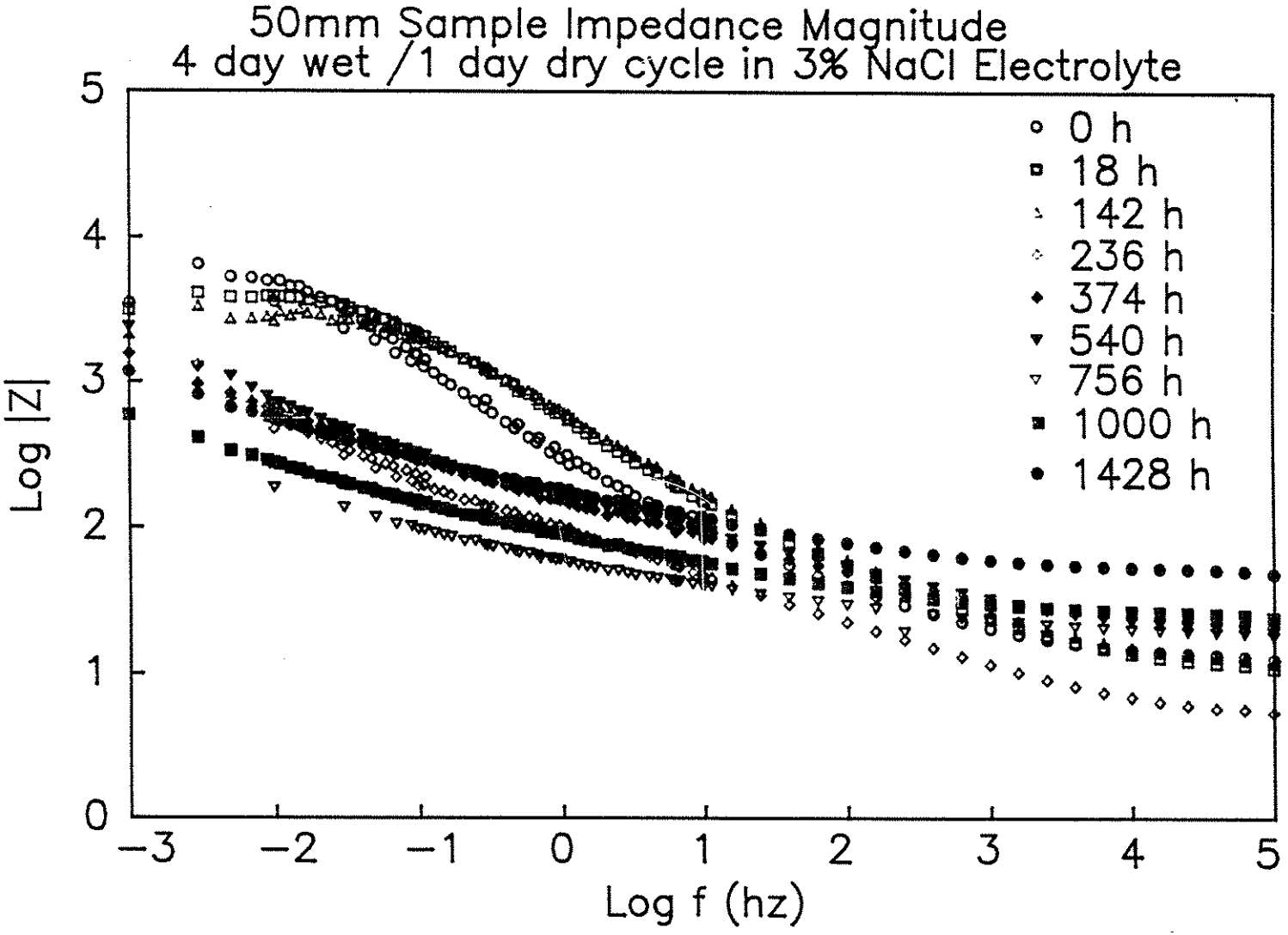

Fig. 10. Impedance magnitude results for a 0.30 mm (12 mil) initial gap specimen subjected to 4/1 (wet/dry) cycles in 3% NaCl solution.

saturated oxide layer were ignored. The characteristics of the early time (0 h) data shown in Fig. 10 that suggest a transmission line model are the lack of sharp corner frequencies at the transitions in slope, and the less than purely capacitive response at an intermediate frequency. Corner frequencies are those at which regions of a Bode plot experience a change in slope. The corner frequency is estimated by the intersection of the extrapolated line from the capacitive region and the line from the resistive region. An example is shown in Fig. 7.

The data for 18 and 142 h may be discussed together because they maintain the same basic characteristics as the time 0 data. The slightly capacitive behavior at intermediate frequencies and resistive behavior at high and low frequencies are still apparent. The high frequency resistive behavior shown for the three sets of data between 0 and 142 h indicates virtually no change in solution resistance. The lack of major changes in the impedance response in the first 142 h of the study was expected, given the minimal dimensional and visual changes observed in crevices with this initial gap. The low frequency region over this same time interval indicated a more substantial decrease in resistivity. At an elapsed time of 142 h, the low frequency resistance is 2800 Ω, less than 50% of the time 0 resistance of 6500 Ω. This value represents the combined resistances in the system. Because the solution resistance term presumably did not change over this time interval, the pore, transfer or leakage resistance must have fallen. From the observed development of active sites in tubercle-like ridges during the first drying cycle, it may be assumed that more active sites decreased these resistances. The formation of a number of active paths through the oxide during the first drying cycle increased the area of the pores in the oxide and decreased the net pore resistance. Or, as described by Macdonald and Park,

$$R_{pore} = P_s \times n \times L/(L-\theta) \times A$$

P_s = pore solution resistivity

n = number of pores

θ = area covered by oxide

A = area of oxide

L = oxide thickness

The observed increase in the number of pores (n) without a major increase in the thickness of the bulk oxide in the crevice will decrease the net pore resistance. Notice that as n increases, the area covered by the oxide term increases by a factor of the pore area. The observed increases in the size of the pits in the tubercle-like ridges decreased the area covered by oxide and presumably also decreased the resistance of the pores.

The data in Fig. 11 show that as the crevice experiences the high corrosion rates associated with a decrease in the solution resistance, the corrosion products begin to fill the crevice and start to impede passage of the electrolyte. The high slopes of the curves in the early time intervals (Fig. 4) show this aggressive corrosion. The decrease in the rate of dimensional change as a function of time represents a decrease in the rate of corrosion in the crevice.

The most severe dimensional changes occurred in specimens with initial gap settings about 0.30 mm (12 mils). Larger crevices were unable to be filled with corrosion product and the smaller crevices were filled with corrosion product at an early stage. Fig. 12 shows the solution resistance as a function of time for a range of initial gap settings. The time 0 data from each of the plots demonstrate the expected effect of the volume of the crevice on the resistance of the solution. The small crevices limit the volume of solution available for transmitting current and have demonstrably higher

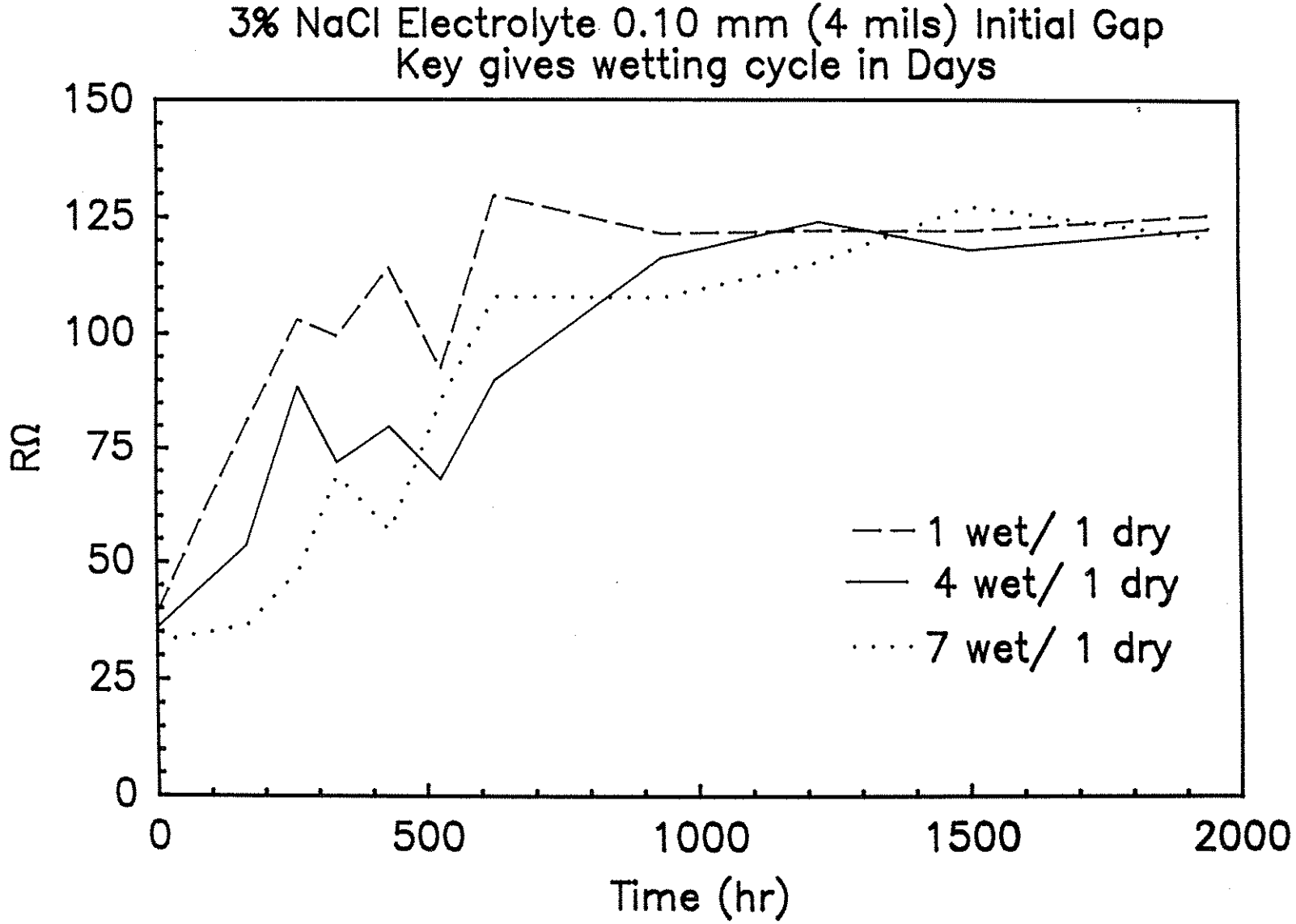

Fig. 11. Solution resistance as a function of time for similar specimens subject to different wet/dry cycles.

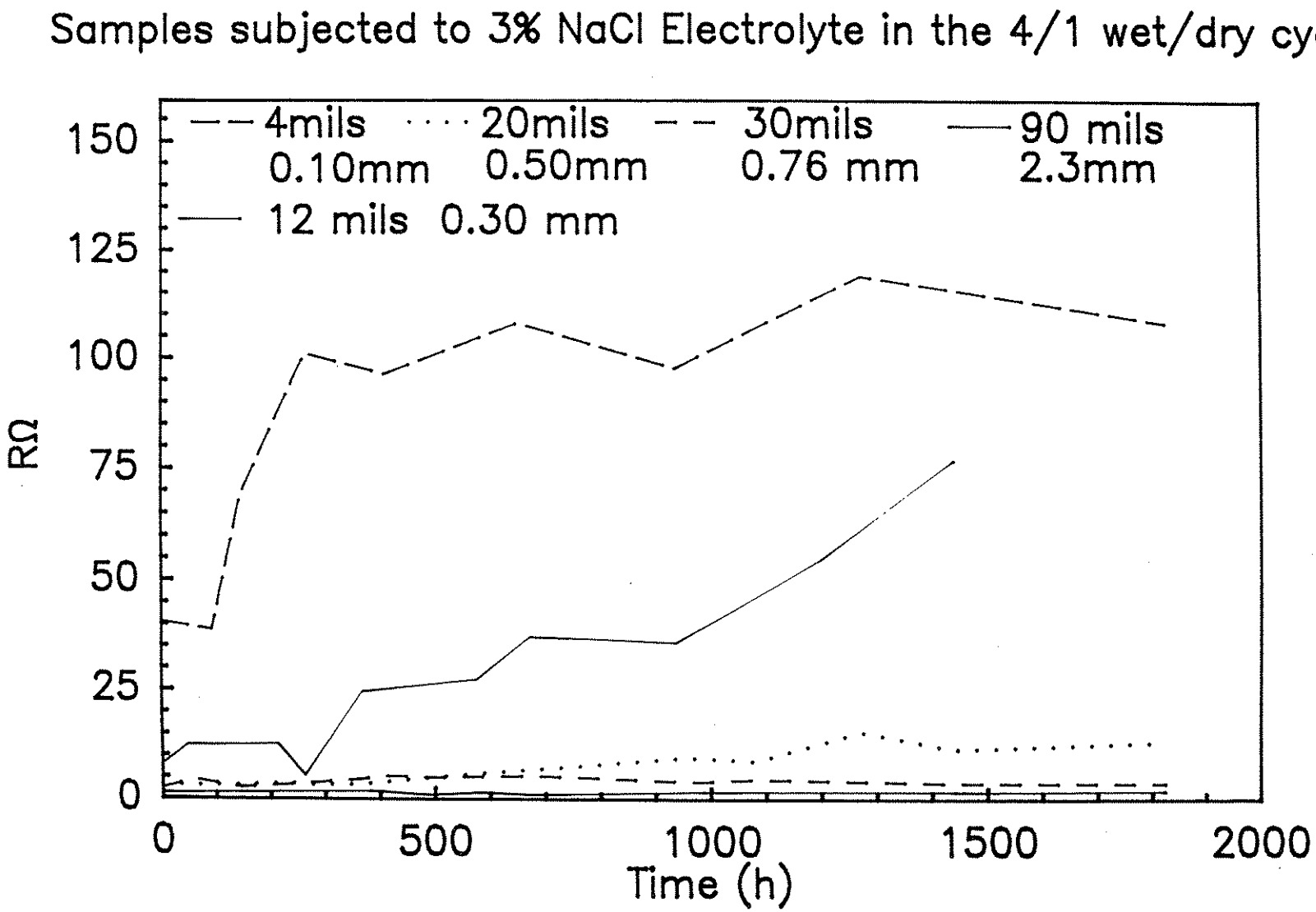

Fig. 12. Solution resistance as a function of time for a variety of initial gap settings.

resistances than the larger gap crevices. This effect is apparent in the ordering of the values for R_{Ω}. There was little change in the resistance of the solution in the larger gap crevices, 2.3 mm and .76 mm (90 and 30 mils) as shown in Fig. 12. Because corrosion packout was never severe in these larger gap crevices, the lack of change in the resistance in the crevice was anticipated. The larger gap crevices never built up enough corrosion product in the crevice to experience a major change in the solution resistance.

Fig. 11 shows that the wetting cycles are important in determining the solution resistance in the first 1000 h of exposure. Over the first 500 h of this experiment the solution resistance for the 1 day/1 day wet/dry cycle rapidly increased. This effect was anticipated from the photographic record, since the most severe corrosion occurred during the drying cycles. Again, the fluctuations in the data due to the wet/dry cycling are apparent. After 500 h, the plots for the specimens all trend together at a solution resistance value of approximately 125 ohms. The photographic record and the impedance observations are consistent. Once the crevice was effectively filled with mass transport inhibiting oxide, the electrolyte access to the crevice was limited and all of the crevices exhibited a similar solution resistance.

The data in Fig. 11 do not indicate if cycles or time is the key factor in the rate of corrosion product evolution in the crevice. The number of cycles in the first 500 h for the frequently wet specimen is four times greater than the number of cycles for the least frequently wet specimen. Yet, both of the specimens trend to the same solution resistance value at around 1000 h. The similarity in the three plots in Fig. 11 after 800 h suggests that the build-up of corrosion product in the crevice causes the drying time to become greater than 7 days. Thus, beyond 800 h each crevice remained in a wet condition.

Figs. 13 A-C show the pH results for 1000 h for gap settings in the range of 0.12-0.30 mm. The increase in the pH for all of these samples has been attributed by Alavi and Cottis [7] and Turnbull [6] to the cathodic reduction of oxygen in the crevice and the formation of OH^- ions. The current flow data for the 0.30 mm (12 mil) gap setting over the first 100 h, as shown in Fig. 14 for 3% NaCl confirms the cathodic reactions in the crevice. Notice that the initial current flow in Fig. 14 is strongly positive. Positive current flows in this section are arbitrarily defined as current flow into the crevice, i.e., the opposite of crevice corrosion. Similar data were obtained for distilled water and a 0.25 mm (10 mil) gap. Although the magnitudes of the pH and current shifts in the distilled water case were lower than in 3% NaCl, the trends were the same. In the early period of the experiment, the crevice did not suffer crevice corrosion. Electrons flowed from the outer cylinder to the core of the crevice, resulting in crevice protection. This crevice protection effect was frequently observed to a lesser degree over the course of the experiments after the sample had been wet for an extended period.

The beginning of a drying cycle is accompanied by a current spike. Notice in Figs. 15 and 16 that these current spikes are negative values. Negative values signify electron flow to the outer segment of the specimen. Thus, a negative current value on any of the plots in this section signifies that the electrode at the center of the crevice core is acting as the anode.

Fig. 15 is an excellent example of crevice acidification in a 3% NaCl trial. Notice in this figure that the drying cycle is accompanied by current spikes in the negative direction. Notice also that these current spikes correlate well with a decrease in the crevice pH. This figure is representative of data from the 3% NaCl trials over time intervals beyond the 100 h range shown above. The same trend was observed in distilled water (Fig. 16)

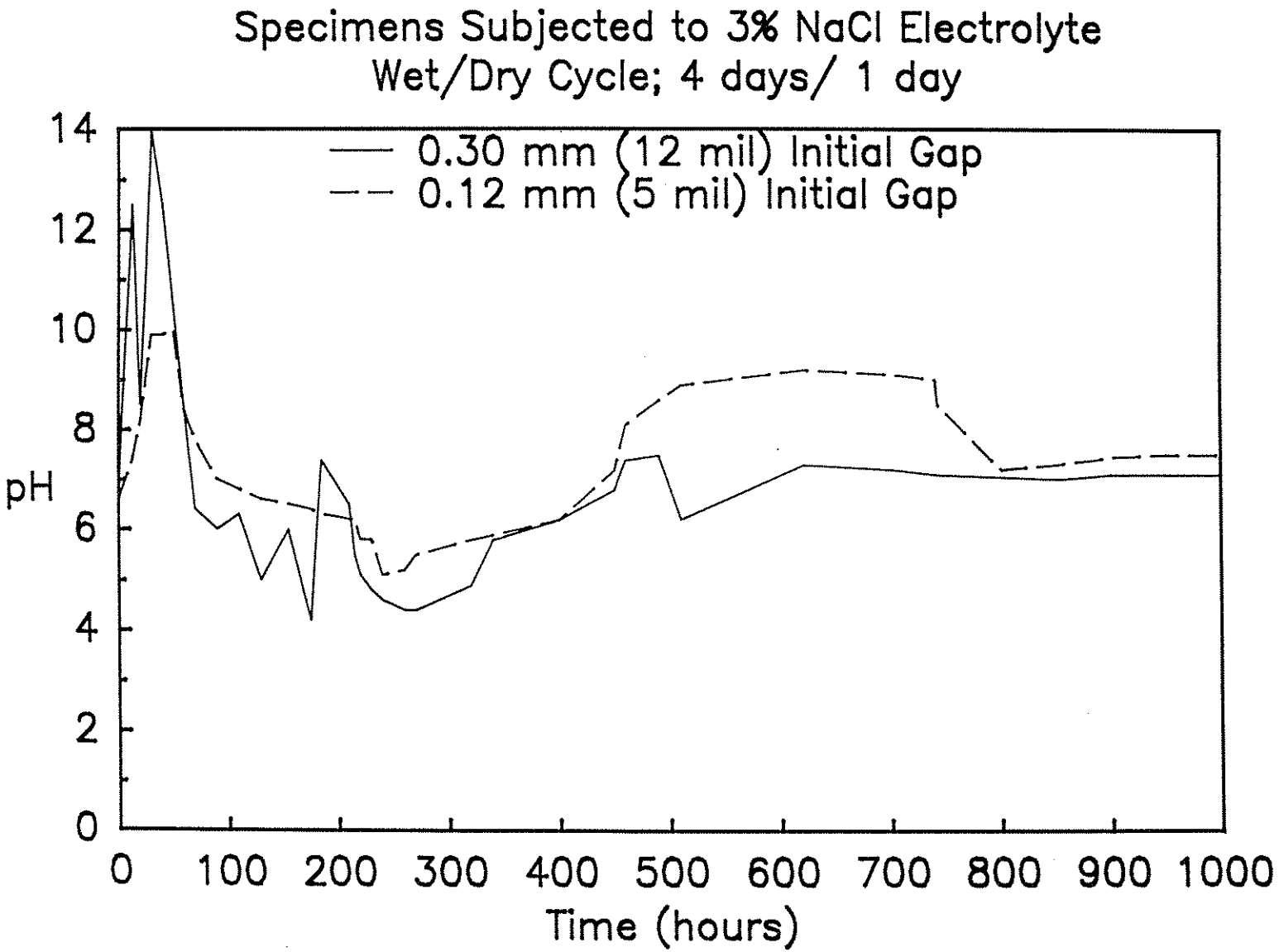

Fig. 13A. Crevice solution pH as a function of time for specimens with different initial gap settings subjected to 3% NaCl electrolyte.

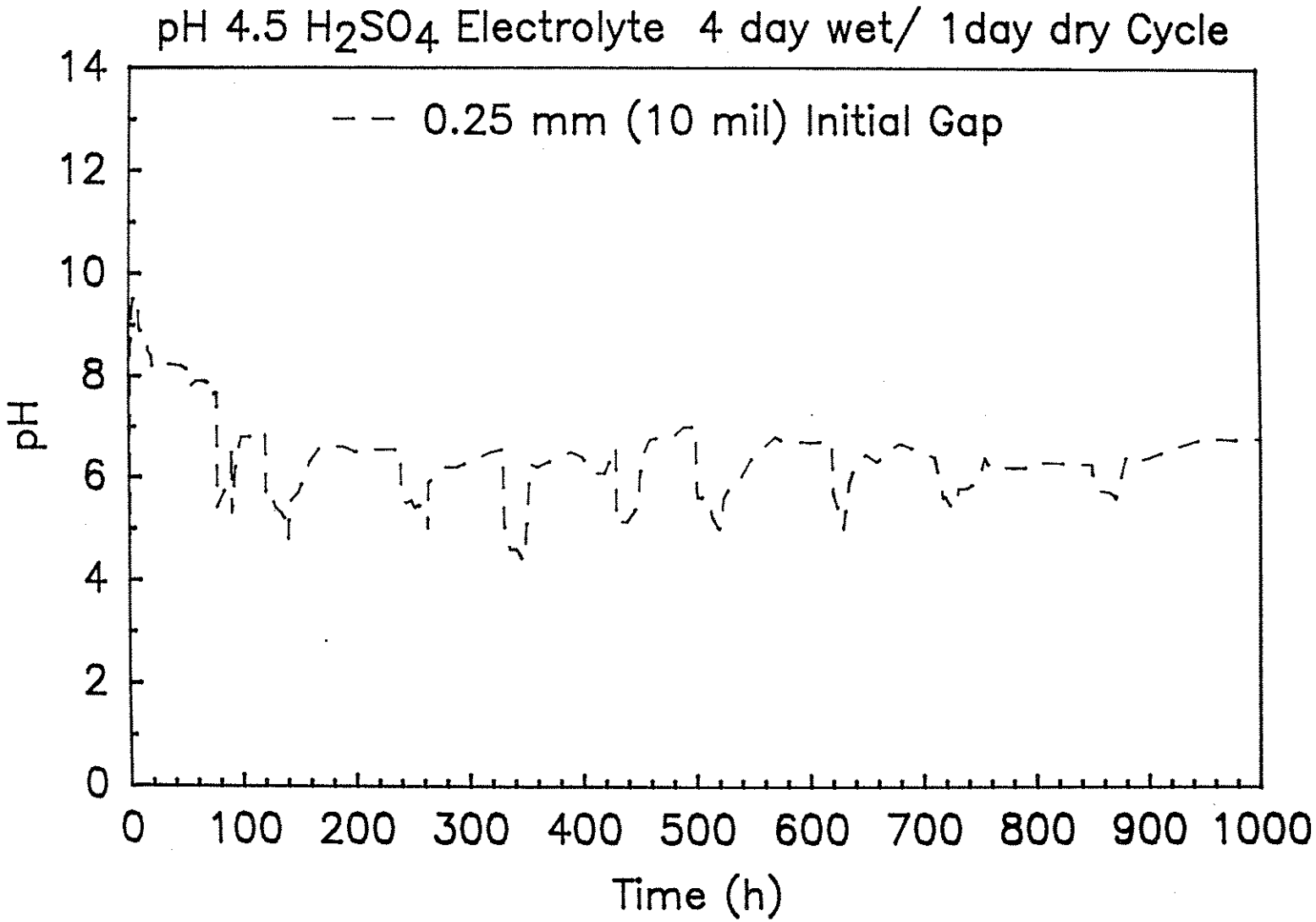

Fig. 13B. Crevice solution pH as a function of time for a specimen subjected to pH 4.5 H_2SO_4 solution.

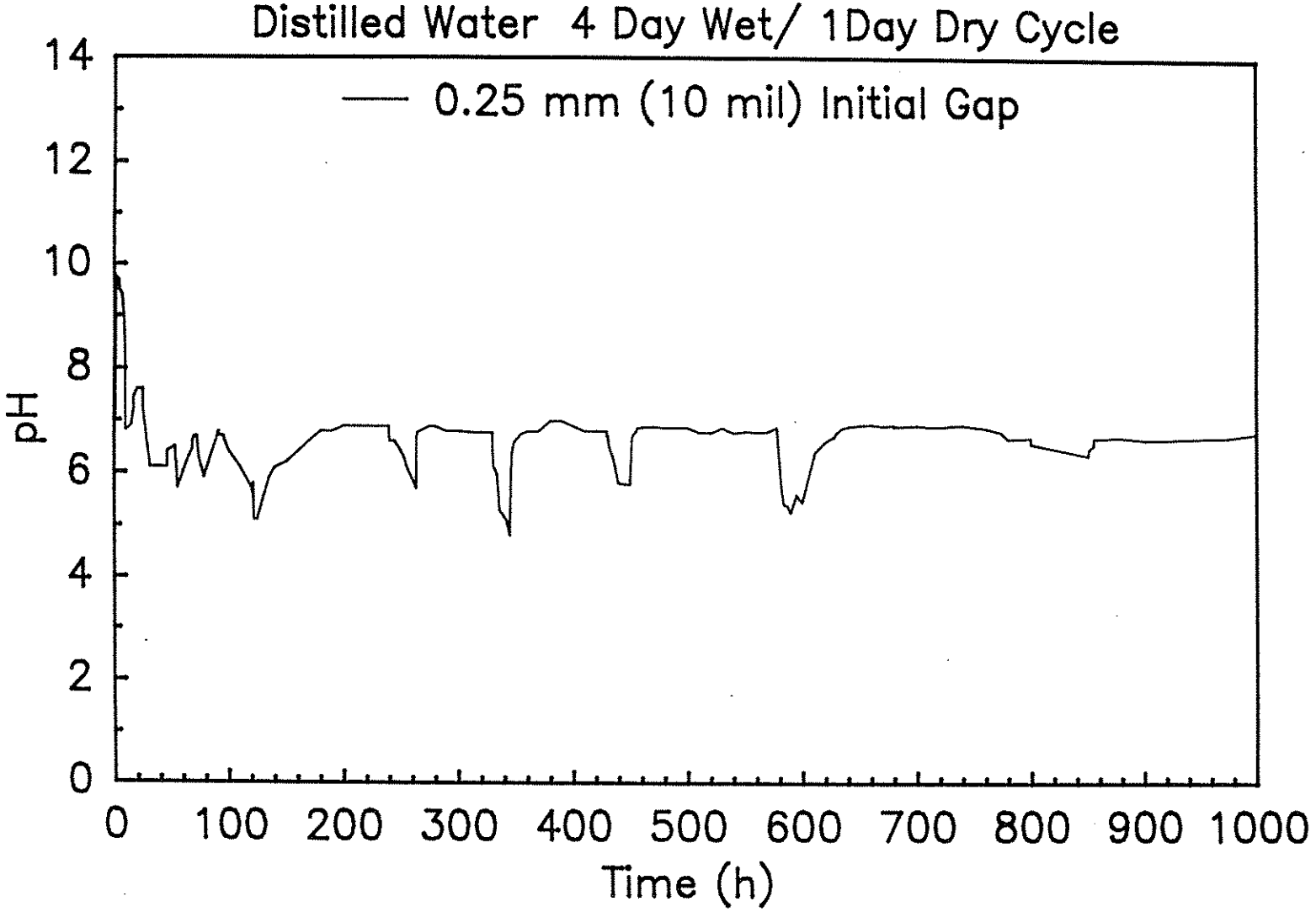

Fig. 13C. Crevice solution pH as a function of time for a specimen subjected to distilled water.

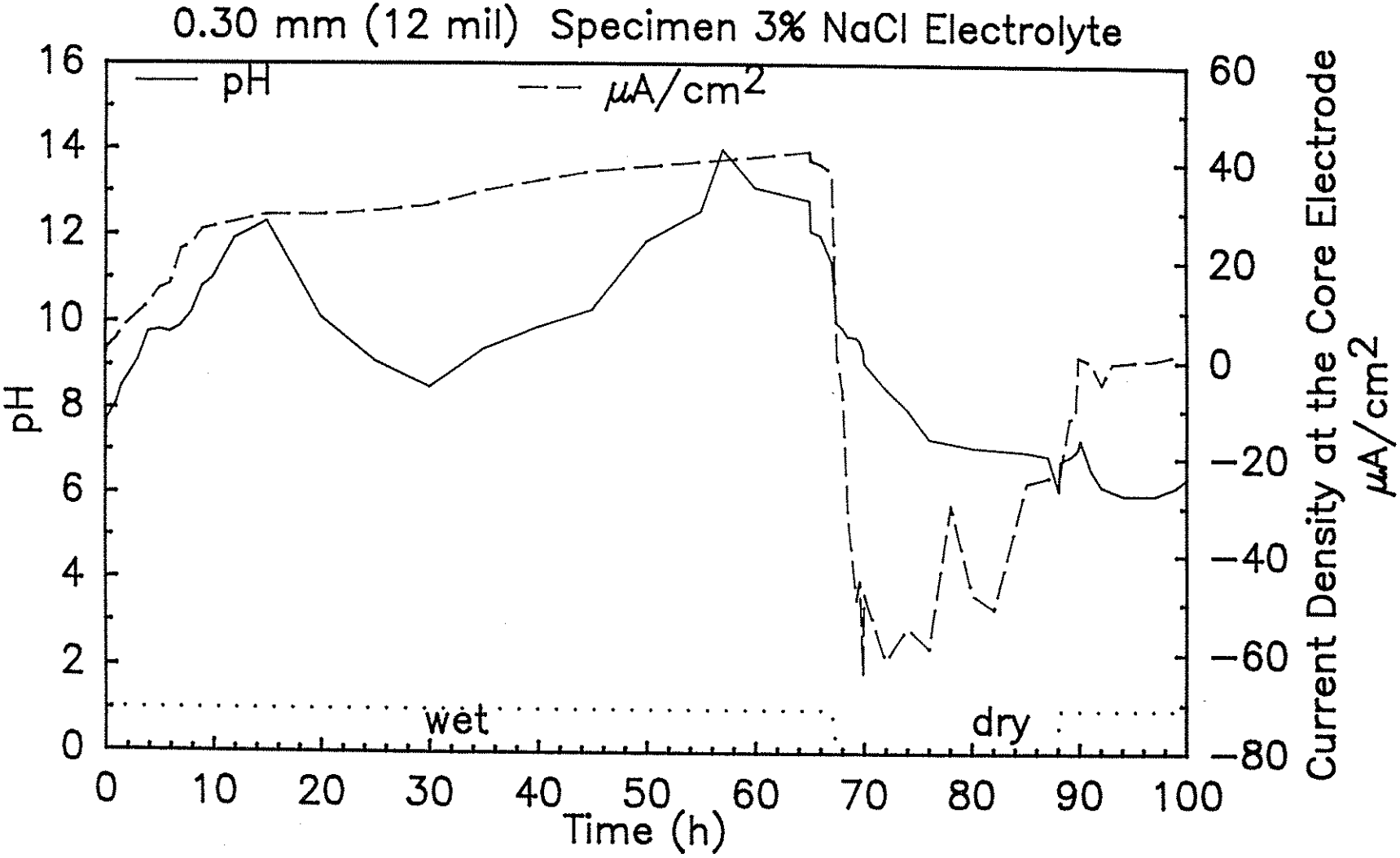

Fig. 14. Potential and current, as a function of time for a 0.30 mm (12 mil) specimen in 3% NaCl electrolyte.

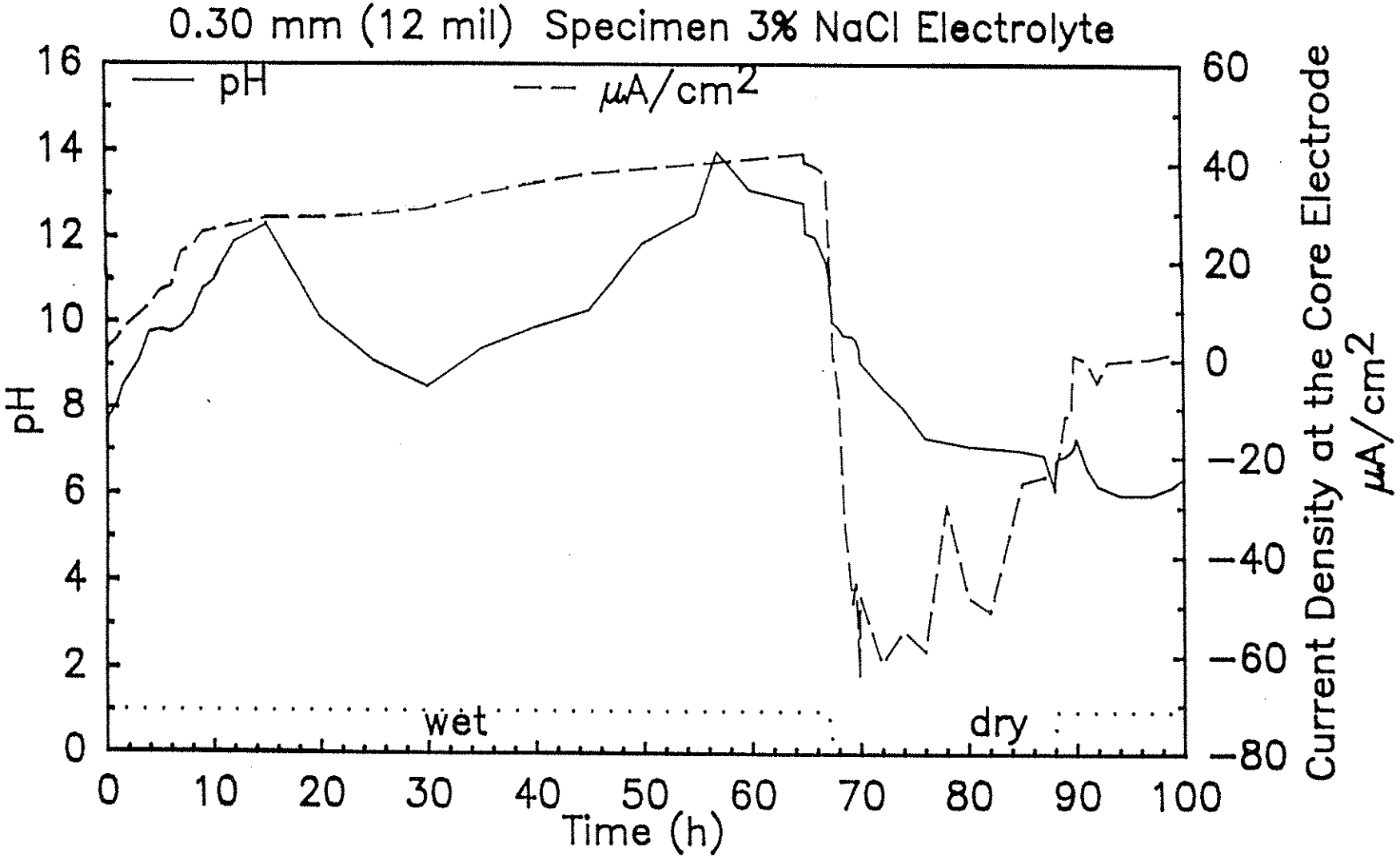

Fig. 15. Current and potential as a function of time for a 0.30 mm (12 mil) specimen subjected to 3% NaCl electrolyte.

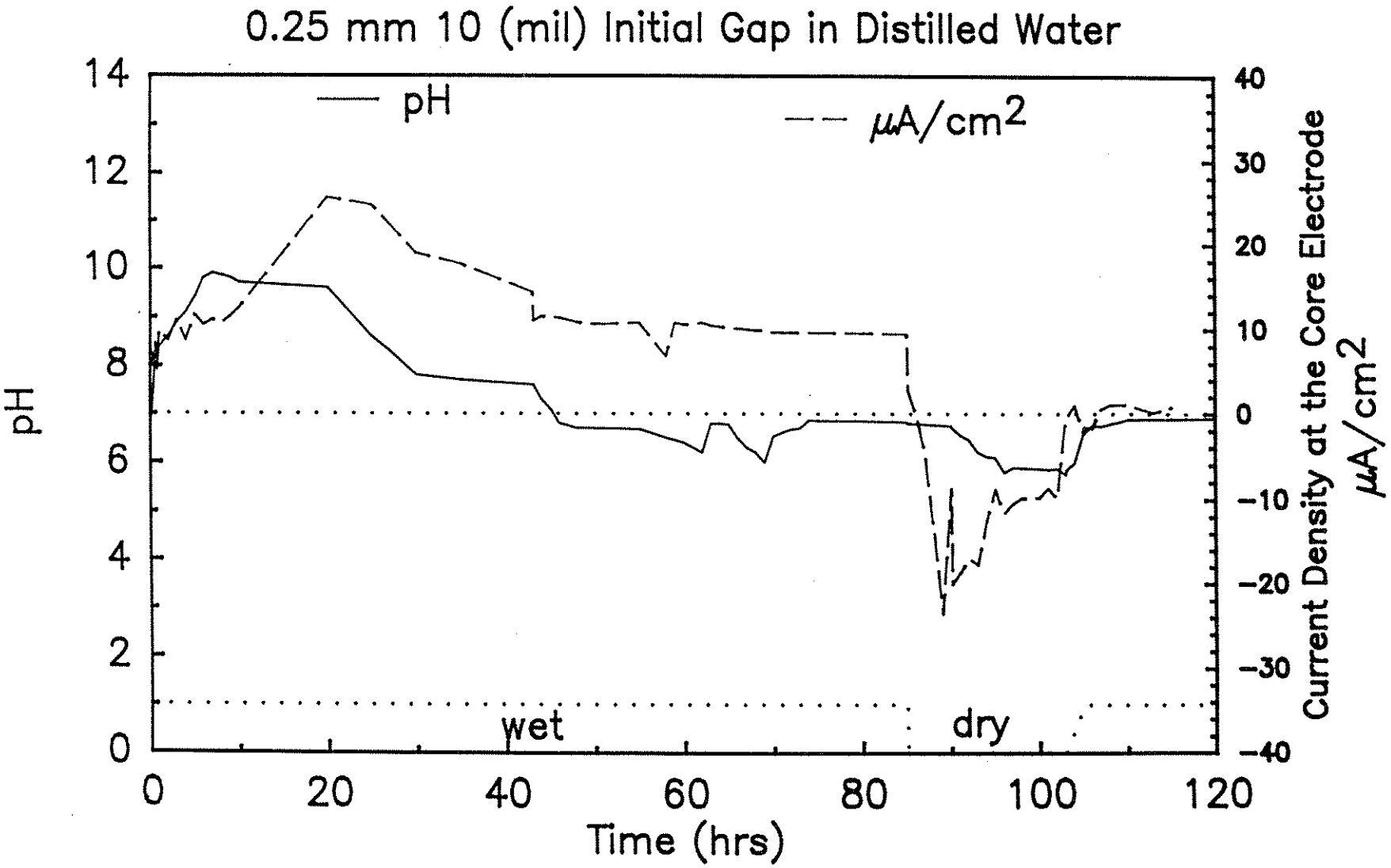

Fig. 16. pH and current as a function of time for a 0.25 mm (10 mil) specimen subjected to distilled water.

and pH 4.5 sulfuric acid.

The current spikes, signifying anodic behavior at the crevice core and cathodic behavior on the external steel segment, as noted in Fig. 15, may be explained by the cathodic reactions on the outer steel segment of the apparatus during the drying cycle. When the solution is withdrawn, a thin layer of water is left in contact with the corrosion products on the outer segment. The atmospheric oxygen access to this thin layer of solution promotes the cathodic oxygen reduction reaction on the outer segment. Because the geometric surface area of this outer region is much larger than the surface area of the crevice core (inner segment), which does not have access to atmospheric oxygen until the drying begins to effect the solution trapped in the crevice, the crevice corrosion rate is very high. Using the instantaneous corrosion rate as determined from the current spike shown in Fig. 16, the corrosion rate may be determined to be equivalent to a metal loss of 4.7×10^{-6} g of metal per cm^2 during the interval of high crevice current flow. This value is extrapolated to a yearly corrosion rate of 0.84 g per cm^2. This severe corrosion rate attests to the severity of the crevice attack during the drying cycle. It is apparent from Fig. 14 that these significant current flows decreased sharply when the external steel surface dried.

After the outer region of the crevice has dried, the cathodic reactions promoted by the atmospheric oxygen must move into the crevice zone. Inside the crevice, only the outer zone of the trapped liquid will interact with the atmosphere and experience cathodic reactions. Because the geometry of the drying zone in the crevice controls the area of this cathodic reaction, the corrosion current in this stage is variable. However, because the surface area of the external segment inside the crevice is only six times larger than the surface area of the core segment, the expected current flow and corrosion rate at this point are lower.

The rewetting of the specimen caused the steel segment at the crevice core to become more anodic than the outer steel segment. The increase in the magnitude of the current flow between the two segments during rewetting is caused by the reactivation of the cathodic sites on the outside of the crevice by the oxygenated electrolyte. The crevice core does not dry totally, so only some portion of the fresh oxygenated solution entering the crevice promotes the cathodic reactions.

The electrolyte in contact with the outer segment of the cell is exposed to the atmosphere and should contain enough oxygen to promote the cathodic reactions. Figures 14-16, however, show the crevice current returning to approximately zero current flow a short time after the crevice is rewet. A zero net current flow does not mean the crevice has stopped corroding but rather that the reaction is under localized control. The assumption that the internal and external crevice electrodes are still corroding actively even when no current flows between them are supported by the findings of Wilde [12]. The profile of the crevices formed by two plates in Wilde's study revealed corresponding zones of attack and protection inside a crevice. The zones of attack in the crevice were assumed to be local active sites, the unattacked zones inside the crevice were assumed to be local cathodes. Wilde found these local attack and protection sites on both sides of his crevice assembly. The occurrence of these sites inside the crevice proves that corrosion can continue in a crevice in the absence of a couple with an external cathode. SEM studies confirmed the observations of Wilde.

The drop in the current flow after the initial high corrosion rate experienced during the rewetting cycle may be partially due to the condition of the residual electrolyte in the crevice when the sample is rewet. The pH data in Figs. 14 and 15 show a decrease in the pH during the drying cycle, followed by an increase in pH during the rewetting phase. A pH of 4.0

suggests that during the drying cycle the increased oxygen access to the electrolyte in the crevice leads to the formation of Fe^{+++} ions. If the assumption is made that some of the Fe^{++} ions in the electrolyte during a drying cycle react with oxygen to form Fe^{+++}, the hydrolysis of these ions with the formation of H^{+} ions explains the observed low pH [13].

After the sample is rewet, the pH begins to trend back towards more neutral values. The trend towards neutral pH values is a consequence of the mixing of the rewetting solution and the residual acidic crevice solution. When the specimen is rewet, fresh cathodic sites on the outside of the samples are exposed to oxygen-rich solution, while the core electrode is exposed to an aggressive acidic solution. The resulting corrosion rate is high for a short time. As the mixing of the fresh electrolyte with the acid electrolyte proceeds, the pH in the crevice becomes neutral and the current flow decreases.

The crevices exposed to 3% NaCl all start to trend towards neutral near the end of the experiment at 1000 h. The magnitudes of the current and pH excursions for the 1000-1800 h time period are not as great as those at shorter times. This effect shown is attributed to the observed packing of the crevice with corrosion products after 1000 h.

ACKNOWLEDGEMENT

Support for this research was provided by the National Science Foundation under an Engineering Research Center grant to Lehigh University.

REFERENCES

[1] R. Oltra and M. Keddam, Corrosion Science 28(1), 1 (1988).

[2] J. W. Fisher and U. Yuceoglu, "A Survey of Localized Cracking in Steel Bridges," Fritz Laboratory Report 448.2, Lehigh University, 1981 (1978).

[3] J. W. Fisher and A. W. Pense, "Final Report on the Mianus River Bridge, Material, Fracture Surface, and Specifications Test for Zetlin Argo Structural Investigations and The Connecticut Department of Transportation," NTSB Report No. PB 84916203, June 1984.

[4] R. L. Brokenbrough, Amer. Inst. of Steel Construction Engrg J., First Quarter 1983, p. 42.

[5] F. P. Ijsseling, Brit. Corr. J 15(2), 51 (1980).

[6] A. Turnbull, Corrosion Science 23(8), 833 (1983).

[7] A. Alavi and R. A. Cottis, "The Measurement of pH, and Chloride Concentration in a Simulated Crevice," AIME Proceedings, Embrittlement by the Localized Environment, Ed. R. P. Gangloff, 1984, pp.75.

[8] D. C. Silverman and A. S. Krisher, "Design Considerations for Occluded Cell Corrosion Monitoring," ASTM STP 908, Eds. G. C. Moran and P. Labine, Philadelphia, PA, 1986, pp.472-91.

[9] R. Alkire, T. Tomasson and K. Hebert, J. Electrochem. Soc. 132(5), 1027 (1985).

[10] R. W. Hertzberg, Deformation and Fracture of Engineering Materials, 2nd Ed., John Wiley & Sons: New York, 1983, pp.642.

[11] D. D. Macdonald and J. R. Park, Corrosion Science 23(4), 295 (1983).

[12] B. E. Wilde, "The Role of Stray Currents in the Corrosion of Bolted Joints of COR-TEN Steel," United States Steel Technical Report, Dec. 1975.

[13] H. Leidheiser, Jr., R. D. Granata, G. Fey and M. Ingle, Corrosion Science 28, 631 (1988).